Effect of Residual Stress on Fracture Behavior by Cohesive Zone Modeling

X.B. Ren[1], Z.L. Zhang[1], B. Nyhus[2]
[1]*Norwegian University of Science and Technology, Trondheim, Norway;*
[2]*SINTEF Materials and Chemistry, Trondheim, Norway*

1. Introduction

Residual stresses have significant effect on the crack-tip constraint [1, 2], which can further influence the fracture toughness of materials. Understanding how residual stresses influence the fracture behavior becomes more and more important when high strength steels are increasingly utilized in offshore industry.

Panontin and Hill [3] investigated the effect of residual stresses on the micromechanics of fracture initiation and found that the residual stress reduced the brittle fracture toughness significantly. They also pointed out that the reduction of the brittle fracture toughness is due to the change of the crack-tip constraint conditions caused by the residual stresses. Hill and Panontin [4] employed the RKR [5] failure theory to predict the brittle fracture for three-point bending samples with and without residual stresses. Their results showed that the residual stress affects both the crack driving force and the crack-tip constraint, and together these effects decrease the fracture toughness.

In this study, a modified boundary layer (MBL) model has been used to investigate the effect of the residual stress on fracture resistance. The residual stress was introduced by so-called "eigenstrain" method. Results showed that the residual stress reduces both the initiation fracture toughness and fracture resistance significantly. It is found that the effect of residual stress is more significant for larger *T-stress.* The effect of residual stress on the fracture resistance also dependents on the material hardening.

2. Numerical procedure

This study concerns an ideal problem. A large round cylinder with a "spot" weld in the center was investigated. The cylinder was simulated by a modified boundary layer model with the remote boundary conditions controlled by the elastic *K-field* and *T-stress,* which has the following form:

$$u(r,\theta) = K_I \frac{1+v}{E} \sqrt{\frac{r}{2\pi}} \cos\left(\frac{1}{2}\theta\right)(3-4v-\cos\theta) + T\frac{1-v^2}{E} r\cos\theta$$

$$v(r,\theta) = K_I \frac{1+v}{E} \sqrt{\frac{r}{2\pi}} \sin\left(\frac{1}{2}\theta\right)(3-4v-\cos\theta) - T\frac{v(1+v)}{E} r\sin\theta$$

(1)

where $K_I = \sqrt{EJ/1 - v^2}$ under plane strain condition; E is Young's modulus, v is Poisson's ratio; r and θ are polar coordinates centered at the crack tip with $\theta = 0$ corresponding to the crack tip; T represents the *T-stress*.

The simulations were performed by ABAQUS/CAE. The analyses were carried out under model I, plain strain conditions. The MBL model used for this study consists of a weld-metal region located in the center of the model and an outer base-metal region, and a sharp crack was assumed in the center of weld-metal region. The radius of the MBL model was taken as 4000mm to ensure that the small scale yielding condition is fulfilled. A layer of uniform size (0.1mm) cohesive element is placed on the central line behind the crack tip to simulate the crack initiation and propagation. The length of the cohesive elements layer is 4.8 mm. The weld- and base-metal region of the model was meshed by standard four-node elements with reduced integration, CPE4R, with finer mesh in the crack-tip region. The cohesive zone is meshed by standard cohesive element COH2D4. The behavior of the cohesive elements is described by a bi-linear traction-separation law, which is characteristic of brittle materials [6]. The maximum traction stress σ_{max} and the fracture energy Γ_0 are two important parameters to characterize the traction-separation-law. The finite element model has 5397 elements and the meshes are shown in Fig.1.
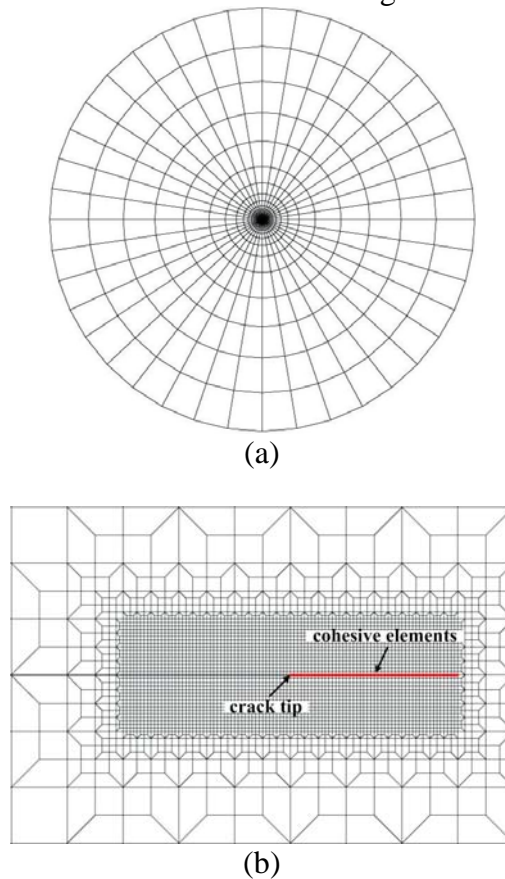

(a)

(b)

Fig.1. Modified boundary layer model, (a) global mesh; (b) crack-tip mesh.

The base-metal and the weld-metal were assumed to have the same elastic properties ($E = 2.07 \times 10^5$ MPa, $\upsilon = 0.3$) and plastic properties. It should be noted that the mismatch between the base-metal and the weld-metal was not taken in account. Rate-independent power law strain hardening materials were used, which have the form of

$$\sigma_f = \sigma_0 \left(1 + \frac{\overline{\varepsilon}^{\,p}}{\varepsilon_0} \right)^n \tag{2}$$

where n is the strain hardening exponent; σ_f is the flow stress; $\overline{\varepsilon}^{\,p}$ is the equivalent plastic strain; σ_0 is the yield stress, $\varepsilon_0 = \sigma_0/E$ is the yield strain, where E is the Young's modulus. The Poisson's ratio is 0.3, Young's modulus E is 207, 000 MPa, yield stress is 460 MPa, which corresponds to a typical modern pipeline steel.

The residual stress field was introduced into the model by so-called eigenstrain method that was also called "inherent strain" method when first introduced by Ueda [7]. The basic idea of eigenstrain method is that the source of residual stress is an incompatible strain field caused by plastic deformation, thermal strains and phase-transformation etc. [8]. Thus, if the distribution of the eigenstrain is known, the distribution of residual stresses can be obtained through linear elastic calculation by using the finite element method. In this study, the eigenstrain values were assumed to be equal to the thermal expansion coefficients of two regions (α_w and α_b), respectively. The residual stresses were then introduced by loading the model with a unit temperature change. Fig.2 presents the redistributed residual stress after the crack was introduced for the case with eigenstrain $\alpha_w = 0.003$ and $\alpha_b = 0$. The stress components were normalized by the yield stress, and the distance from the crack tip was normalized by the radius of the weld metal region c.
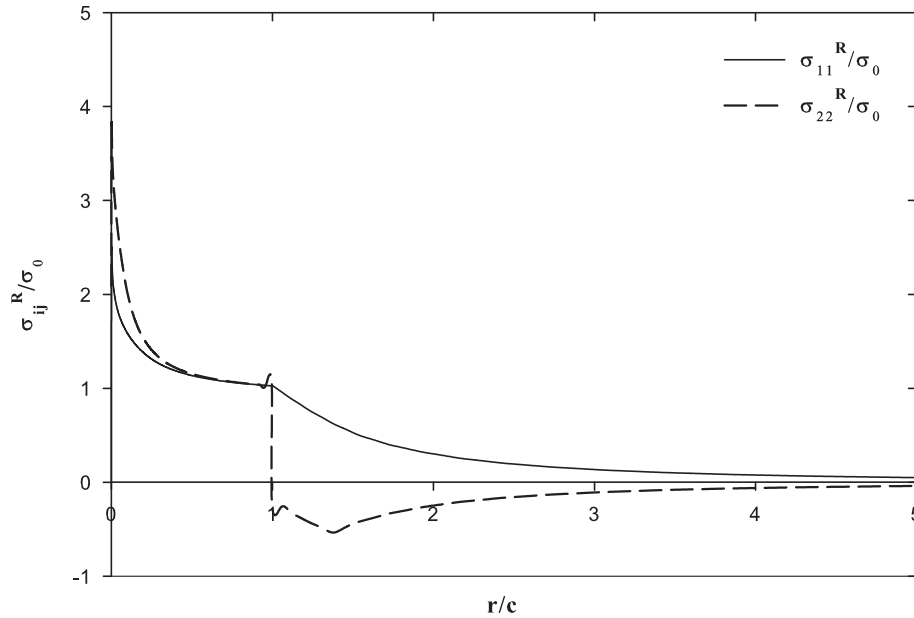
Fig.2. Residual stress field introduced by the eigenstrain method.

It can be seen that the residual stresses along both the parallel and opening directions have a sharp turning point at the interface of the base-metal and weld-metal. The reason for the sharp turning point is that the assumed distribution of the eigenstrain is not continuous between the two regions. It can also be seen that both the parallel and opening residual stresses in the weld metal are tensile. In the base-metal region, the residual stress parallel to the crack plane is also tensile in a large range while the opening residual stress is compressive to counter balance the tensile stress in the weld-metal.

3. Results and discussion

Fracture is sensitive to the near tip stress field. There is no or negligible plastic deformation before failure for brittle materials. The effect of residual stress on the fracture resistance was investigated in this study. It should also be noted that the *J-integral* was adopted as the measure of the crack driving force. The computed *J-integral* by ABAQUS shows practically path-independence beyond the large strain region for the cases investigated.

3.1 Effect of residual stress on fracture resistance

In order to study the effect of the residual stress on the initiation and the propagation of the crack, the fracture resistance curve for the cases with and without residual stress effect are compared in Fig 3. Three residual stress cases

4

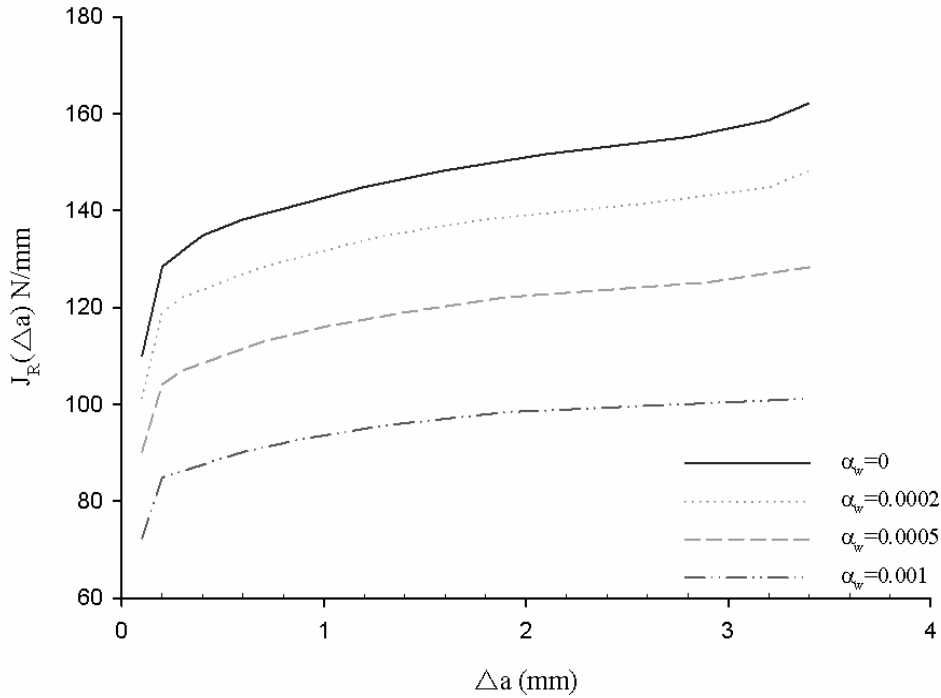were analyzed, and the fracture resistance curves start when the first cohesive element failed.

Fig.3. Fracture resistance curves of the case with and without residual stresses. $E/\sigma_0 = 450$, $\upsilon = 0.3$, $n = 0.1$; Cohesive energy $\Gamma_0 = 100$ N/mm, and the maximum stress $\sigma_{max} = 3\sigma_0$. The solid curve with $\alpha_w = 0$ corresponds to the case without residual stress.

It can be seen that the residual stresses reduce the initiation fracture toughness significantly. Also, with the increasing of the residual stresses, the fracture resistance curve shifted downwards. The opening stress plays an important role for cleavage fracture. In our previous work [2], a crack-tip constraint parameter R was defined based on the difference of the opening components between the reference field (small-scale-yielding solution without residual stresses) and the full stress field including the residual stress at the position $r/(J/\sigma_0) = 2$. It was found that a higher level residual stress field induced higher crack-tip constraint. Thus, the reduction of fracture resistance in Fig.3 may be explained as the crack-tip constraint increasing caused by the residual stresses.

3.2 Effect of the residual stress on the fracture resistance for materials with different hardening components

The material properties may also influence the residual stress-induced crack-tip constraint [2]. In this study, the effect of the residual stress on the fracture resistance curve was also investigated for three hardening components, as shown

5

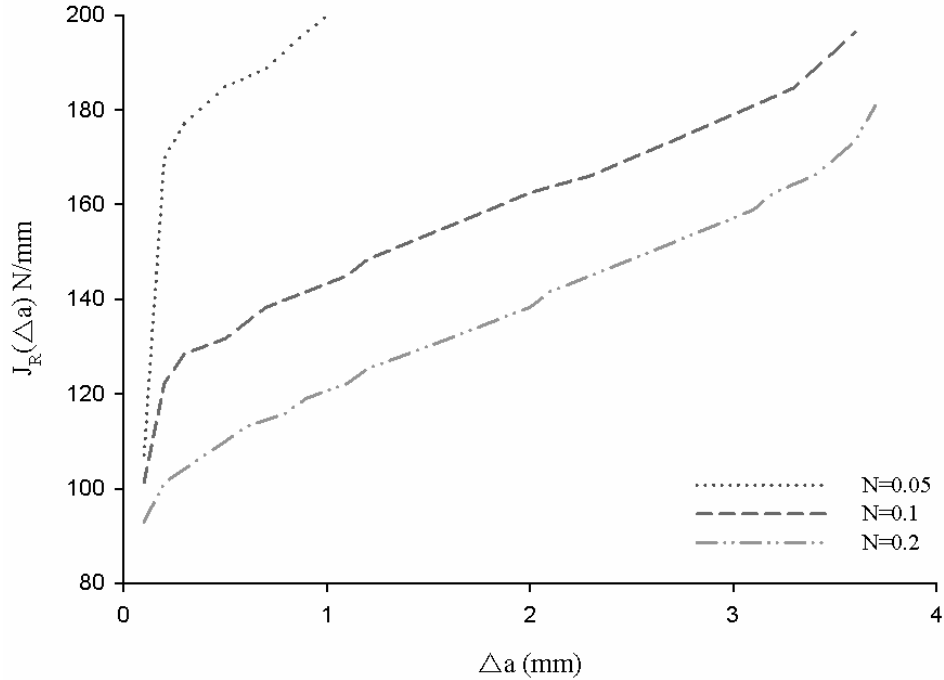in Fig. 4. It should be noted that the same residual stress field of $\alpha_w = 0.002$ was used.

Fig.4. Fracture resistance curves with different values of *N* for the same residual stress field. $E/\sigma_0 = 450,\ \upsilon = 0.3;\ \Gamma_0 = 150$ N/mm; $\sigma_{max} = 3\sigma_0$.

It can be seen that the fracture resistance curve is lower for the material with the larger hardening component. Our previous study showed that the residual stress-induced crack-tip constraint is higher when the material hardening component is larger [2], which may causes a lower fracture resistance curve as shown in Fig.4.

3.3 Effect of the residual stress on the fracture resistance with different T-stress

It is interesting to investigate the effect of the residual stress on the fracture resistance curves for different *T-stresses*. As showed in Section 2, the remote displacement field of the MBL model is controlled by the elastic *K-field* and *T-stress* applied at the round boundary. By changing the *T-stress*, different crack-tip constraint conditions can be obtained. In this study, the cases of $T/\sigma_0 = 0.5,\ 0$ and -0.5 were studied. The same residual stress field of $\alpha_w = 0.0005$ was introduced. The fracture resistance curves of both with and without residual stress under three *T-stress* cases are plotted in Fig.5
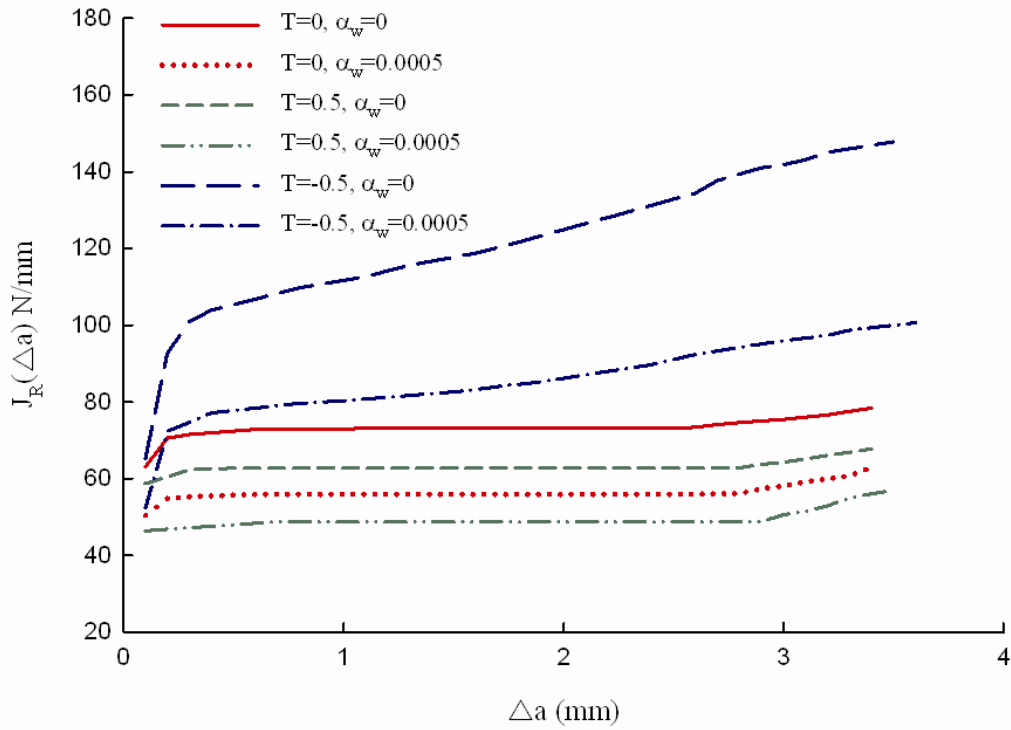
Fig.5. Fracture resistance curves of both with and without residual stress cases under different *T-stress*. $E/\sigma_0 = 450$, $\upsilon = 0.3, n = 0.1$; $\alpha_w = 0.0005$; the cohesive energy $\Gamma_0 = 50$ N/mm.

It can be seen that the effect of residual stress on the fracture resistance is stronger for smaller *T-stress*. It is also interesting to find that the reduction of the fracture resistance caused by the residual stress is approximately same for $T/\sigma_0 = 0.5$ and $T/\sigma_0 = 0$. However, the difference is relatively large for T=-0.5 case. Results in [2] indicated that the effect of the residual stress is weaker for higher geometry constraint condition, which can probably explain the result in Fig.5.

4. Concluding remarks

In this study, the effect of residual stress on fracture resistance is studied by cohesive zone modeling under mode I, plane stain conditions. The modified boundary layer simulations are performed with the remote boundary conditions controlled by the elastic *K-field* and *T-stress*. The eigenstrain method is used to introduce a two-dimensional tensile residual stress field near the crack tip.

It is found that the residual stress reduces both the initiation fracture toughness and fracture resistance significantly. With the increasing of the residual stress field, the fracture resistance curves move downwards. The residual stress-induced

crack-tip constraint can explain the effect on fracture toughness. The residual stress affects the fracture resistance more significantly under lower geometry constraint condition. The fracture resistance seems lower for higher hardening component materials when the same residual stress field was introduced.

Acknowledgement

References

[1] J. Liu, Z.L. Zhang and B. Nyhus, Residual stress induced crack-tip constraint, Eng. Fract. Mech. 75 (2008) 4151-4166

[2] X. B. Ren, Z.L. Zhang and B. Nyhus, Effect of residual stress on the crack-tip constraint in a modified boundary layer model. (Submitted to Int. J. Solids Struct.)

[3] T. L. Panontin and M. R. Hill, The effect of residual stresses on brittle and ductile fracture initiation predicted by micromechanical models, Int. J. F Fract. 82 (1996) 317-333

[4] M. R. Hill and T. L. Panontin, Effect of Residual Stress on Brittle Fracture Testing, Fatigue and Fracture Mechanics: 29th Volume, ASTM STP, (1994), 1321

[5] R. O. Ritchie, J. F. Knott and J.R. Rice, Relationship between critical tensile stress and fracture toughness in mild steel, J. Mech. Phys. Solids. 21 (1973) 395-410

[6] A. Cornec, I. Scheider and K.H. Schwalbe, On the practical application of the cohesive model, Eng. Fract. Mech. 70 (2003)1963-1987

[7] Y. Ueda, K. Fukuda, K. Nakacho and S. Endo, A new measuring method of residual stresses with the aid of finite element method and reliability of estimated values, Trans. Japan Welding Research Institute 4(2) (1975)123-131

[8] M.R. Hill and D.V. Nelson, The inherent strain method for residual stress determination and its application to a long welded joint, Structural Integrity of Pressure Vessels, Piping, and Components ASME **318** (1995), pp. 343–352.